AD-A167 019 CALCULATION OF SINGLE- AND DOUBLE-PHOTON FREE-FREE CROSS SECTIONS FOR ELE..(U) NEW YORK UNIV NY DEPT OF PHYSICS E J ROBINSON FEB 86 AFWAL-TR-85-2115 1/1

UNCLASSIFIED F33615-80-C-2049 F/G 20/8 NL

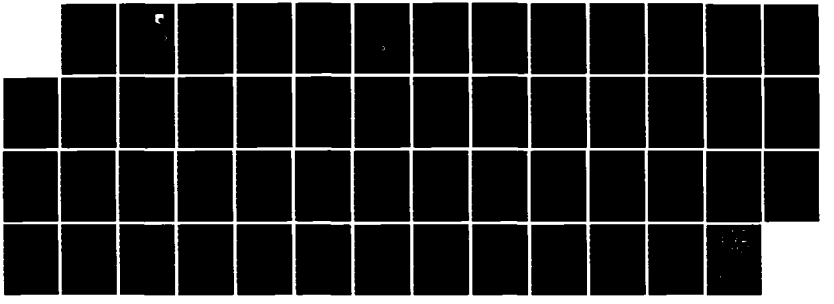

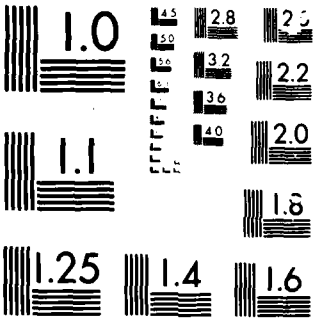

MICROCOPY CHART

(2)

AFWAL-TR-85-2115

CALCULATION OF SINGLE- AND DOUBLE-PHOTON FREE-FREE CROSS SECTIONS FOR ELECTRONS SCATTERED FROM HE, C, N, NE AND AR

Professor Edward J. Robinson
Department of Physics
New York University
New York, New York 10003

February 1986

FINAL REPORT FOR PERIOD September 1980 - February 1983

Approved for Public Release; Distribution is Unlimited

AERO PROPULSION LABORATORY
AIR FORCE WRIGHT AERONAUTICAL LABORATORIES
AIR FORCE SYSTEMS COMMAND
WRIGHT-PATTERSON AIR FORCE BASE, OHIO 45433

NOTICE

When Government drawings, specifications, or other data are used for any purpose other than in connection with a definitely related Government procurement operation, the United States Government thereby incurs no responsibility nor any obligation whatsoever; and the fact that the government may have formulated, furnished, or in any way supplied the said drawings, specifications, or other data, is not to be regarded by implication or otherwise as in any manner licensing the holder or any other person or corporation, or conveying any rights or permission to manufacture use, or sell any patented invention that may in any way be related thereto.

This report has been reviewed by the Office of Public Affairs (ASD/PA) and is releasable to the National Technical Information Service (NTIS). At NTIS, it will be available to the general public, including foreign nations.

This technical report has been reviewed and is approved for publication.

Charles A. DeJoseph, Jr.

CHARLES A. DEJOSEPH, JR.
Physicist, Power Components Branch
Aerospace Power Division
Aero Propulsion Laboratory

William G. Seward

WILLIAM A. SEWARD, Maj, USAF
TAM, Power Components Branch
Aerospace Power Division
Aero Propulsion Laboratory

FOR THE COMMANDER

James D. Reams

JAMES D. REAMS
Chief, Aerospace Power Division
Aero Propulsion Laboratory

"If your address has changed, if you wish to be removed from our mailing list, or if the addressee is no longer employed by your organization please notify AFWAL/POOC-3 *W-PAFB, OH 45433 to help us maintain a current mailing list".*

Copies of this report should not be returned unless return is required by security considerations, contractual obligations, or notice on a specific document.

UNCLASSIFIED

SECURITY CLASSIFICATION OF THIS PAGE

AD-A167019

REPORT DOCUMENTATION PAGE

1a. REPORT SECURITY CLASSIFICATION Unclassified	1b. RESTRICTIVE MARKINGS
2a. SECURITY CLASSIFICATION AUTHORITY	3. DISTRIBUTION/AVAILABILITY OF REPORT Approved for public release, distribution is unlimited
2b. DECLASSIFICATION/DOWNGRADING SCHEDULE	
4. PERFORMING ORGANIZATION REPORT NUMBER(S)	5. MONITORING ORGANIZATION REPORT NUMBER(S) AFWAL-TR-85-2115
6a. NAME OF PERFORMING ORGANIZATION New York University 6b. OFFICE SYMBOL (If applicable) Physics	7a. NAME OF MONITORING ORGANIZATION Aerospace Power Division Aero Propulsion Laboratory (AFWAL/POOC-3)
6c. ADDRESS (City, State and ZIP Code) 4 Washington Place New York NY 10003	7b. ADDRESS (City, State and ZIP Code) Air Force Wright Aeronautical Labs Wright-Patterson AFB OH 45433-6563
8a. NAME OF FUNDING/SPONSORING ORGANIZATION AF Office of Scientific Research 8b. OFFICE SYMBOL (If applicable) AFOSR/NP	9. PROCUREMENT INSTRUMENT IDENTIFICATION NUMBER F33615-80-C-2049
8c. ADDRESS (City, State and ZIP Code) Bolling AFB DC 20332	10. SOURCE OF FUNDING NOS. PROGRAM ELEMENT NO.: 66102F; PROJECT NO.: 2301; TASK NO.: S2; WORK UNIT NO: 82
11. TITLE (Include Security Classification) Calculation of Single & Double Photon Free Free Cross Sections (over)	
12. PERSONAL AUTHOR(S) Edward J. Robinson	
13a. TYPE OF REPORT Final 13b. TIME COVERED FROM 09/80 TO 02/83	14. DATE OF REPORT (Yr., Mo., Day) February 1986 15. PAGE COUNT 56
16. SUPPLEMENTARY NOTATION	

17. COSATI CODES		
FIELD	GROUP	SUB GR
20	3	24
20	6	15

18. SUBJECT TERMS (Continue on reverse if necessary and identify by block number)
Electron scattering, Free-free radiation, perturbation theory, frequency dependence

19. ABSTRACT (Continue on reverse if necessary and identify by block number)

Calculations of cross sections for the free-free absorption of radiation by electrons scattered from atoms are reported. The results apply in the limit where theory is valid, and are obtained in the context of a realistic independent particle atomic model, which facilitates numerical solutions for both perturbed and unperturbed wave functions. Both one-photon and two-photon absorptions are analyzed, the latter in a mixed gauge representation.

The method is applied to several different atomic targets--the ground states of He, for frequencies corresponding to the $^3S_1$ and $^1S_0$ states of He, for frequencies corresponding to the carbon dioxide, neodymium, and ruby lasers. The low-frequency results agree well with the soft-photon approximation, while, as one might expect, the numbers at shorter wavelengths diverge. For all cases, it was found that the free-free cross sections were negligibly small compared to radiationless cross sections, for intensities no greater than 10^6 W/cm^2.

20. DISTRIBUTION/AVAILABILITY OF ABSTRACT UNCLASSIFIED/UNLIMITED [X] SAME AS RPT [ ] DTIC USERS [ ]	21. ABSTRACT SECURITY CLASSIFICATION UNCLASSIFIED
22a. NAME OF RESPONSIBLE INDIVIDUAL Charles A. DeJoseph, Jr.	22b. TELEPHONE NUMBER (Include Area Code) (513) 255-2923 22c. OFFICE SYMBOL AFWAL/POOC-3

DD FORM 1473, 83 APR EDITION OF 1 JAN 73 IS OBSOLETE.

UNCLASSIFIED

SECURITY CLASSIFICATION OF THIS PAGE

Block 11. Title (Continued)

for Electrons Scattered From He, C, N, Ne and Ar

FOREWORD

This report describes an effort conducted by personnel of the Department of Physics, New York University, under Contract F33615-80-C-2049.

The work reported herein was performed during the period 1 September 1980 to 28 February 1983, under the direction of the author, Dr. Edward J. Robinson, Principal Investigator.

The work was performed with the collaboration of Dr Robin Shakeshaft, Dr Anatoly Grinberg, and Mr Chaik Chang. The author wishes to thank Mr Charles DeJoseph for several valuable suggestions.

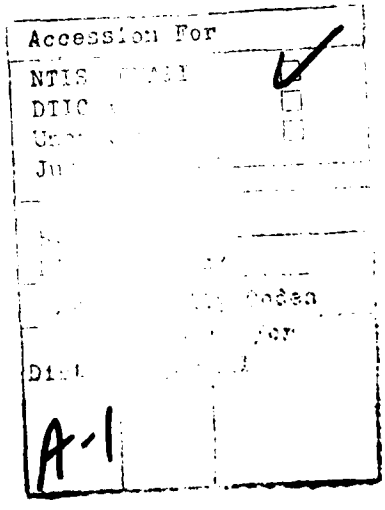

TABLE OF CONTENTS

LIST OF TABLES

SECTION I

INTRODUCTION

Over the past decade, considerable interest has developed in the problem of free-free radiative transitions of electrons scattered by atomic or molecular targets (Refs. 1-5). Part of the motivation arises from experiment, and part from the realization that at low frequencies, one may relate the scattering amplitude in the presence of radiation to the corresponding parameter without the field. That is, the radiative scattering amplitude for soft photons is a combination of terms, each of which is a product of a field-free amplitude and a factor which is a function of field and the momentum of the projectile. No further knowledge of electronic wave functions is needed to calculate transition probabilities. Thus, if one were primarily interested in calculating cross-sections, it would not be necessary to engage in analysis much more detailed than in the field-free case, although to be as accurate as possible, one should use T-matrix elements that do not lie on the energy shell.

The soft-photon approximation may be regarded from another point of view as well. Off-shell T-matrix elements are not, by definition, accessible to direct measurement. Since they enter into the formulas of the soft-photon approximation, however, one could imagine performing a set of experiments to measure free-free cross sections which could be used to deduce the off-shell T-matrix elements. Thus, the role of the radiative problem could be understood as a probe to gather data for the field-free scattering.

In the present report, we are mainly interested in the actual calculation of cross sections for photo-induced processes, whether or not the soft-photon approximation holds, and shall use perturbation theory as our main calculational tool. A by-product of our work is an accessment of the limits of validity of the soft-photon approximation. In addition, we have checked our codes against the soft-photon approximation, in the regime of intensities and frequencies where both it and perturbation should be valid.

SECTION II

THEORETICAL BACKGROUND

Throughout this report, we shall assume that the material system is excited by a single mode laser field, which we shall treat classically, since we are concerned with an intensity range where transition probabilities calculated via semiclassical radiation theory are indistinguishable from the results of quantum electrodynamics. We shall also assume the dipole approximation to be valid, an assumption entirely justified for wavelengths large compared to atomic dimensions. The interaction between the field and the electrons may be equally well represented by the three forms

$$H' = -\underline{E} \cdot \underline{r}, \tag{1}$$

$$H' = -\underline{A} \cdot \underline{p}/mc + e^2A^2/2mc^2, \tag{2}$$

$$H' = e\underline{Z} \cdot \text{grad } V(\underline{r})/mc^2 + e^2(\underline{Z} \cdot \text{grad})^2 V(\underline{r})/2m^2c^4 + e^2A^2/2mc^2, \tag{3}$$

where $\underline{E}$ is the electric field, $\underline{A}$ the vector potential, and $\underline{Z}$ the Hertz vector. The three forms of the interaction are denoted as the length, velocity, and acceleration gauges, respectively. The function $V(\underline{r})$ is the unperturbed potential in which the electrons move. The three forms are equivalent to withir unitary transformations, although in particular applications, one or another may be more convenient to use. We shall have occasion to calculate single and double photon matrix elements of these operators. To the lowest allowed orders of perturbation theory, these are, in the length, velocity, and acceleration gauges, respectively,

$$M_{1L} = -e\ (\phi_f\ \underline{E}\cdot\underline{r}\ \phi_o), \tag{4}$$

$$M_{1v} = (-e/mc)\ (\phi_f\ \underline{A}\cdot\underline{p}\ \phi_o), \tag{5}$$

$$M_{1a} = (e/mc^2)\ (\phi_f\ \underline{Z}\ \text{grad}\ V\ \phi_o), \tag{6}$$

$$M_{2l} = e^2\ S\ (\phi_f\ \underline{E}\cdot\underline{r}\ \phi_k)\ (\phi_k\ \underline{E}\cdot\underline{r}\ \phi_o)/D_w, \tag{7}$$

$$M_{2v} = (e^2/m^2c^2)\ S\ (\phi_f\ \underline{A}\cdot\underline{p}\ \phi_k)\ (\phi_k\ \underline{A}\cdot\underline{p}\ \phi_o)/D_w, \tag{8}$$

$$M_{2a} = (e^2/m^2c^4)\ S\ (\phi_f\ \underline{Z}\ \text{gradV}\ \phi_k)\ (\phi_k\ \underline{Z}\ \text{gradV}\ \phi_o)/D_w + (e^2/2m^2c^4)\ (\phi_f\ (\underline{Z}\ \text{grad})^2V\ \phi_o). \tag{9}$$

The energy denominator D_w is given by $E_o - E_k \pm \hbar\omega + i\epsilon$, where it is understood that we are to take the limit as the positive parameter ϵ approaches zero. This explicitly incorporates the "outgoing" nature of the Green's function into the problem. One uses the plus sign for absorption, the minus for emission. Note that the term proportional to A^2 in the velocity and acceleration interaction Hamiltonians does not contribute to two-photon transitions in the dipole approximation.

It is also possible to write the two-photon matrix element in a "mixed" gauge representation, i.e., one in which one of the matrix elements in the product is in the velocity gauge and the other in the acceleration gauge. The two-photon matrix element in the mixed gauge is given by

$$M_{2m} = (e^2/2\ m^2c^2)\ S\ ((\phi_f|\underline{Z}.\text{gradV}|\phi_k)(\phi_k|\underline{A}\cdot\underline{p}|\phi_o) + (\phi_f|\underline{A}\cdot\underline{p}|\phi_k)(\phi_k|\underline{Z}\cdot\text{gradV}|\phi_o))/D_w. \tag{10}$$

In these equations, ϕ_o, ϕ_k, ϕ_f denote the initial, intermediate, and final state wave functions, and S represents a sum over all intermediate states, including an integration over the continuum.

In calculations of free-free matrix elements for single-photon processes, there is a certain advantage to using the acceleration gauge, which involves calculating radial integrals of operators of asymptotic form

r^{-n}, where n is at least two. In our realistic model (Refs. 6 and 7), n = 5. Since the radial wave functions behave like r^{-1} as r increases, the integrals converge easily. This is not so for the length and velocity forms, for which the integrands go like r^1 and r^0, respectively, as r grows without bound. To determine these integrals, it is necessary to first evaluate numerically the contribution from r = 0 to r = R, where R is large, but finite. At R, the radial wave functions have assumed their asymptotic forms. By inserting a convergence factor into the integrands, the integration from R to infinity may be performed analytically. The convergence factor usage may be justified on physical grounds--it corresponds to integrating over all momentum components in the final state wave function. While this device formally removes the divergence, it frequently happens that the analytic and numerical portions of the integration almost exactly cancel, so that one is left with the difference between two almost identical terms, a remainder notoriously subject to numerical errors. This cancellation is a residue of the case of V = 0, where the cross section for free-free processes does vanish, so that the cancellation must be exact.

One might expect to find it similarly advantageous to use the acceleration form of the two-photon matrix element. In this case, though, there is an additional complication, namely the term proportional to Z^2. This contribution generates two drawbacks--for low frequencies, it may almost exactly cancel the term second-order in $\underline{Z}$ gradV, imposing an accuracy requirement on the two parts similar to that discussed above. In addition, for realistic Coulombic potentials, the Z^2 term generates a delta-function contribution, which mandates accurate knowledge of the wave

function at the origin. It is well-known that the wave function at the origin is unreliable in numerical and approximate calculations, so that considerable care must be exercised if one wishes to use the acceleration gauge for two-photon rates.

It turns out that the advantages obtained by using the acceleration gauge in single-photon calculations may be transferred to the two-photon case, without suffering the indicate drawbacks, by going over a mixed gauge approach, provided that we perform the analysis in the implicit summation scheme, which we had intended to use anyway. The only price we pay for the mixed gauge approach is in the length of computer time required to complete the computation. We are obliged to double the number of inhomogeneous equations solved.

The matrix elements for second-order processes require that one perform infinite summations over intermediate states. The implicit method enables one to reduce each sum to a single term. For example, in the velocity gauge, we may define

$$\phi_o^{(1)} = S\, \phi_k\, (\phi_k|\underline{A}\cdot\underline{p}|\phi_o)/D_w, \tag{11}$$

so that

$$M_{2v} = (e^2/2m^2c^2)\, (\phi_f|\underline{A}\cdot\underline{p}|\phi_o^{(1)}). \tag{12}$$

The function $\phi_o^{(1)}$ satisfies the inhomogeneous equation

$$(H_o - E_o \pm \hbar w - ie\,)\phi_o^{(1)} = -\underline{A}\cdot\underline{p}\,\phi_o. \tag{13}$$

Alternatively, one could define

$$\phi_f^{(1)} = S\, \phi_k\, (\phi_k|\underline{A}\cdot\underline{p}|\phi_f)/D_w^*, \tag{14}$$

so that

$$M_{2v} = (e^2/2m^2c^2)\, (\phi_f^{(1)}|\underline{A}\cdot\underline{p}|\phi_o), \tag{15}$$

where

$$(H_o - E_o + \hbar w + ie)\, \phi_f^{(1)} = -A\cdot \underline{p}\, \phi_f. \qquad (16)$$

In the mixed representation, we require both $\phi^{(1)}$ functions. The matrix element for two-photon processes becomes

$$M_{2m} = (e^2/2\hbar m^2c^2)((\phi_f|\underline{Z}\cdot \mathrm{grad}V|\phi_o^{(1)})+(\phi_f^{(1)}|\underline{Z}\cdot \mathrm{grad}V|\phi_o)).$$

We solve Eqs. (13) and (16) by separation of variables in the single-particle version of the problem. We write, for example,

$$\phi_o = 4\pi \sum i^L e^{i\eta_L}\, U_L(kr)Y_{LM}(\theta,\phi)Y_{LM}(\theta',\phi')/kr \qquad (17)$$

where θ, ϕ, θ', ϕ', are the polar and azimuthal angles of the electronic coordinate and momentum, and η_L the phase shift for angular momentum L and propagation constant k. The radiation field is assumed to be linearly polarized along the z-axis. Operating on ϕ_o with the interaction operator for the velocity gauge, Ap_z, we find

$$Ap_z\, \phi_o = -i4\pi A \sum i^{L+2}(2L+1)^{-\frac{1}{2}}Y_{LM}(\theta,\phi)\, \Big[e^{i\eta_{L+1}}Y_{L+1,M}(\theta',\phi')$$
$$((L+1)^2-M^2)/2L+3\ ^{\frac{1}{2}}((L+2)U_{L+1}(kr)/r+U'_{L+1}(kr)) + e^{i\eta_{L-1}}$$
$$Y^*_{L-1,M}(\theta',\phi')\ (L^2-M^2)/2L-1\ ^{\frac{1}{2}}((L-1)U_{L-1}(kr)/r-U'_{L-1}(kr)\Big] \qquad (18)$$

It is convenient to define $S_L = rU_L$. The function $\phi_o^{(1)}$ has the expansion

$$\phi_o^{(1)} = \sum P_{LM}(r)\, y_{LM}(\theta,\phi)/r. \qquad (19)$$

The p_{LM} satisfy differential equations of the form

$$(-\tfrac{1}{2}d^2/dr^2 + V(r) + \tfrac{1}{2}L(L+1)/r^2 - \tfrac{1}{2}k^2 \pm \hbar w)\, P_{LM} =$$
$$4\, Ai^{L+2}\, (2L+1)^{-\frac{1}{2}}\ e^{i\eta_{L+1}}\ Y_{L+1,M}(\theta',\phi')((L+1)^2-M^2)/$$
$$(2L+3))^{\frac{1}{2}}\ ((L+!)S_{L+1}(kr)/r + S'_{L+1}(kr)) + e^{i\eta_{L-1}}$$
$$Y^*_{L-1,M}\ (\theta',\phi')((L^2-M^2)/(2L-1))^{\frac{1}{2}}(LS_{L-1}(kr)/r - S'_{L-1}(kr)) \qquad (20)$$

These are solved numerically by the following procedure. For large values of r, the potential V(r) vanishes, and the inhomogeneity assumes its asymptotic form, which is a linear combination of $rj_L(kr)$ and $ry_L(kr)$, where j_L, y_L are spherical Bessel functions of the first and second kinds.

In this region there is a particular solution of the inhomogeneous equation that similarly has the form of a linear combination of $rj_L(kr)$ and $ry_L(kr)$. We numerically integrate this particular solution inward to the origin, where it normally diverges. The singularity is removed by superimposing a multiple of that solution of the corresponding homogeneous equation that exhibits a singularity of the same character as the origin. A multiple of the regular solution is also appended to make the full complementary function satisfy outgoing boundary conditions for large values of r.

A variation of this procedure is used for two-photon calculations with the Kruger-Schulz model (Ref. 8). The inhomogeneous equation technique is a Green's function method. For the K-S model, it is convenient to explicitly calculate the Green's function. In the acceleration gauge, the interaction is non-vanishing only at the discontinuity of the model potential, where it is proportional to the delta function and its derivative. Accordingly, the integrals which define the matrix elements are trivial to evaluate, and involve the Green's function for the case where both spatial arguments are the radius of the square well.

In the perturbative approach to the problem of calculating radiative transition rates, which we have been discussion, one requires, formally at least, the electronic wave function for all separations of the target nucleus and the bombarding electron. At low frequencies, all this information is not needed. One requires, in this limit, only the field-free scattering amplitude, which is equivalent to specifying the wave function only for large separations. That is, the results are insensitive to the short-range details of the solution to the Schrodinger equation. The small-r behavior manifests itself only to the extent that it influences the asymptotic form.

Since the conditions for validity of the soft-photon approximation depend on the wavelength of the radiation but not on its intensity, whether or not the approximation applies to a particular problem is independent of whether perturbation theory may be used. However, since our interest is confined to what is basically a weak-field regime, we shall utilize a perturbative form of the low-frequency approximation--that is, we shall represent the Bessel functions which appear in the expansion of the transition matrix elements by the leading terms in their power series expansions. In practice, we shall always use this perturbative form of the soft-photon approximation, although for convenience we shall retain the full Bessel function in the formal expression for the scattering amplitude. The formula for the T-matrix element for an N-photon process in the soft-photon approximation is given by (Ref. 9)

$$T_{uv}^{(N)} = \sum J_{N-M}(\underline{Q}\cdot\underline{k}_{fv})\, T_{uv}^{RL}(E_i + M\hbar\omega)\, J_M(-\underline{Q}\cdot\underline{k}_{iu}), \qquad (21)$$

where $\underline{Q} = (e/mc\omega)A_0\hat{e}$, $J_M(x)$ is the Bessel function of integer order M, and $\hat{e}$ the unit polarization vector. The symbols u and v denote target states, i and f initial and final, and the superscript RL (radiationless) indicates the corresponding T-matrix element in the absence of the field. We shall also refer to the "extreme" soft-photon approximation, where the variation of T_{uv}^{RL} with energy is ignored.

SECTION III

MODEL POTENTIALS

In our actual calculations, we made use of two classes of potentials--those for which closed-form solutions could be obtained, but which were not representative of real systems, and realistic models which had to be attacked by numerical methods. The former class was investigated to get a qualitative feeling for the problem, while the realistic model was used to generate cross sections.

In the (unrealistic) Kruger-Schulz model, the target atom has two states with energies $E_1 = 0$ and $E_2 = 0.5$ a.u. The electron-target interaction is represented by a 2x2 symmetric matrix $\underline{V}(r)$, defined by

$$\underline{V}(r) = (\hbar^2/2m)\, \underline{U}\, \theta(r-R), \tag{22}$$

where

$$\underline{U} = -a_o^{-2} \begin{bmatrix} 0.06 & 0.04 \\ 0.04 & 0.55 \end{bmatrix}, \tag{23}$$

where a_o is the Bohr radius, θ the step function, and r the distance of the electron from the target, which does not interact with the laser. The choice of the parameter R is arbitrary, of course. We have retained the same $R = 6a_o$ used in the original work of Kruger and Schulz to facilitate comparisons with their results. We emphasize that the problem is solvable in closed form with this model, although computers are used to obtain results from standard representations of analytic function.

The "realistic" potential is the same one used by Robinson and Geltman (Ref. 7) and by Geltman (Ref. 6) to study photo-induced transition rates.

The many-electron system is represented by a single particle interacting with an effective potential which simulates the actual projectile-target interaction. It is taken to be of the form

$$V = V_{HFS} - (e^{-r/r_1} - 1)/r - a_L(e^{-r/r_1} - 1)/2(r^2+r_o^2)^2, \qquad (24)$$

where V_{HFS} is the Hartree-fock-slater potential published by Herman and Skillman (Ref. 10), a_L the polarizability of the target, and r_o and r_1 adjustable parameters. The second term removes the coulomb tail of V_{HFS}, and the third is the polarization potential. We use atomic units for Eq. (24). This potential has been successful in predicting electron scattering cross sections and photodetachment rates (Refs. 7, 8, 11, 12).

Numerical results for free-free absorption cross sections are presented in Tables 1 through 8.

TABLE 1

SINGLE-PHOTON FREE-FREE CROSS SECTIONS FOR ELECTRONS SCATTERED FROM THE METASTABLE STATES OF HELIUM

$E_{phot} = 0.00882$

E_{inc}	E_{fin}	^1S_o (exact)	^1S_o (soft)	$^3S_1$ (exact)	$^3S_1$ (soft)
0.99118	1.0	0.706-1	0.119+0	0.702-1	0.989-1
0.89118	0.9	0.730-1	0.121+0	0.726-1	0.994-1
0.79118	0.8	0.757-1	0.123+0	0.751-1	0.101+0
0.69118	0.7	0.789-1	0.126+0	0.781-1	0.102+0
0.59118	0.6	0.824-1	0.127+0	0.814-1	0.103+0
0.49118	0.5	0.867-1	0.128+0	0.853-1	0.104+0
0.39118	0.4	0.923-1	0.130+0	0.903-1	0.104+0
0.29118	0.3	0.100+0	0.131+0	0.967-1	0.106+0
0.19118	0.2	0.113+0	0.133+0	0.106+0	0.111+0
0.09118	0.1	0.137+0	0.139+0	0.116+0	0.112+0

Table 1. Single-Photon Free-Free Cross Sections for Electrons Scattered from the Metastable States of Helium (Continued)

$E_{phot} = 0.086$

E_{inc}	E_{fin}	^1S_o (exact)	^1S_o (soft)	$^3S_1$ (exact)	$^3S_1$ (soft)
0.914	1.0	0.832-5	0.133-4	0.825-5	0.109-4
0.814	0.9	0.868-5	0.135-4	0.858-5	0.111-4
0.714	0.8	0.911-5	0.138-4	0.897-5	0.112-4
0.614	0.7	0.962-5	0.140-4	0.945-5	0.113-4
0.514	0.6	0.103-4	0.142-4	0.101-4	0.115-4
0.414	0.5	0.111-4	0.145-4	0.108-4	0.116-4
0.314	0.4	0.125-4	0.148-4	0.120-4	0.118-4
0.214	0.3	0.150-4	0.153-4	0.142-4	0.123-4
0.114	0.2	0.218-4	0.166-4	0.198-4	0.135-4

Table 1. Single-Photon Free-Free Cross Sections for Electrons Scattered from the Metastable States of Helium (Continued)

$E_{phot} = 0.1308$

E_{inc}	E_{fin}	^1S_o (exact)	^1S_o (soft)	$^3S_1$ (exact)	$^3S_1$ (soft)
0.8692	1.0	0.165-5	0.250-5	0.161-5	0.204-5
0.7692	0.9	0.172-5	0.254-5	0.169-5	0.208-5
0.6692	0.8	0.182-5	0.259-5	0.178-5	0.210-5
0.5692	0.7	0.194-5	0.264-5	0.189-5	0.214-5
0.4692	0.6	0.211-5	0.271-5	0.206-5	0.216-5
0.3692	0.5	0.237-5	0.278-5	0.228-5	0.222-5
0.2692	0.4	0.276-5	0.288-5	0.264-5	0.228-5
0.1692	0.3	0.365-5	0.312-5	0.344-5	0.246-5

TABLE 2

SINGLE-PHOTON FREE-FREE CROSS SECTIONS

FOR ELECTRONS SCATTERED FROM THE GROUND

STATES OF HELIUM AND NEON

$E_{phot} = 0.00882$

E_{inc}	E_{fin}	He (exact)	He (soft)	Ne (exact)	Ne (soft)
0.99118	1.0	0.354-1	0.353-1	0.267-1	0.272-1
0.89118	0.9	0.331-1	0.330-1	0.239-1	0.242-1
0.79118	0.8	0.305-1	0.304-1	0.209-1	0.212-1
0.69118	0.7	0.276-1	0.275-1	0.181-1	0.183-1
0.59118	0.6	0.244-1	0.244-1	0.153-1	0.156-1
0.49118	0.5	0.208-1	0.208-1	0.126-1	0.127-1
0.39118	0.4	0.169-1	0.169-1	0.996-2	0.101-1
0.29118	0.3	0.127-1	0.127-1	0.738-2	0.748-2
0.19118	0.2	0.826-2	0.826-2	0.481-2	0.489-2
0.09118	0.1	0.381-2	0.382-2	0.220-2	0.226-2

Table 2. Single-Photon Free-Free Cross Sections for Electrons Scattered from the Ground States of Helium and Neon (Continued)

$E_{phot} = 0.086$

E_{inc}	E_{fin}	He (exact)	He (soft)	Ne (exact)	Ne (soft)
0.914	1.0	0.399-5	0.381-5	0.298-5	0.288-5
0.814	0.9	0.374-5	0.354-5	0.264-5	0.254-5
0.714	0.8	0.344-5	0.324-5	0.232-5	0.222-5
0.614	0.7	0.311-5	0.291-5	0.201-5	0.190-5
0.514	0.6	0.274-5	0.253-5	0.169-5	0.159-5
0.414	0.5	0.234-5	0.213-5	0.140-5	0.129-5
0.314	0.4	0.191-5	0.168-5	0.111-5	0.100-5
0.214	0.3	0.144-5	0.120-5	0.823-6	0.715-6
0.114	0.2	0.956-6	0.724-6	0.538-6	0.433-6

Table 2. Single-Photon Free-Free Cross Sections for Electrons Scattered from the Ground States of Helium and Neon (Continued)

$E_{phot} = 0.1308$

E_{inc}	E_{fin}	He (exact)	He (soft)	Ne (exact)	Ne (soft)
0.8692	1.0	0.756-6	0.732-6	0.558-6	0.565-6
0.7692	0.9	0.707-6	0.684-6	0.497-6	0.503-6
0.6692	0.8	0.652-6	0.631-6	0.436-6	0.441-6
0.5692	0.7	0.590-6	0.569-6	0.378-6	0.382-6
0.4692	0.6	0.522-6	0.505-6	0.320-6	0.324-6
0.3692	0.5	0.447-6	0.433-6	0.264-6	0.268-6
0.2692	0.4	0.356-6	0.354-6	0.210-6	0.212-6
0.1692	0.3	0.280-6	0.271-6	0.157-6	0.162-6

TABLE 3

SINGLE-PHOTON FREE-FREE CROSS SECTIONS

FOR ELECTRONS SCATTERED FROM THE GROUND

STATES OF CARBON AND NITROGEN

$E_{phot} = 0.00882$

E_{inc}	E_{fin}	C (exact)	C (soft)	N (exact)	N (soft)
0.99118	1.0	0.952-1	0.957-1	0.725-1	0.725-1
0.89118	0.9	0.879-1	0.883-1	0.661-1	0.662-1
0.79118	0.8	0.798-1	0.802-1	0.595-1	0.596-1
0.69118	0.7	0.710-1	0.713-1	0.523-1	0.525-1
0.59118	0.6	0.613-1	0.616-1	0.448-1	0.451-1
0.49118	0.5	0.509-1	0.511-1	0.369-1	0.372-1
0.39118	0.4	0.398-1	0.401-1	0.286-1	0.289-1
0.29118	0.3	0.283-1	0.284-1	0.202-1	0.206-1
0.19118	0.2	0.167-1	0.169-1	0.119-1	0.122-1
0.09118	0.1	0.634-2	0.648-2	0.552-2	0.581-2

Table 3. Single-Photon Free-Free Cross Sections for Electrons Scattered from the Ground States of Carbon and Nitrogen (Continued)

$E_{phot} = 0.086$

E_{inc}	E_{fin}	C (exact)	C (soft)	N (exact)	N (soft)
0.914	1.0	0.108-4	0.103-4	0.815-5	0.774-5
0.814	0.9	0.995-5	0.941-5	0.745-5	0.703-5
0.714	0.8	0.905-5	0.847-5	0.670-5	0.627-5
0.614	0.7	0.806-5	0.746-5	0.591-5	0.547-5
0.514	0.6	0.700-5	0.635-5	0.508-5	0.463-5
0.414	0.5	0.585-5	0.517-5	0.420-5	0.374-5
0.314	0.4	0.463-5	0.392-5	0.330-5	0.284-5
0.214	0.3	0.336-5	0.265-5	0.238-5	0.192-5
0.114	0.2	0.210-5	0.143-5	0.148-5	0.104-5

Table 3. Single-Photon Free-Free Cross Sections for Electrons Scattered from the Ground States of Carbon and Nitrogen (Continued)

$E_{phot} = 0.1308$

E_{inc}	E_{fin}	C (exact)	C (soft)	N (exact)	N (soft)
0.8692	1.0	0.206-5	0.198-5	0.155-5	0.151-5
0.7692	0.9	0.191-5	0.183-5	0.142-5	0.137-5
0.6692	0.8	0.175-5	0.166-5	0.128-5	0.123-5
0.5692	0.7	0.156-5	0.148-5	0.114-5	0.109-5
0.4692	0.6	0.137-5	0.128-5	0.986-6	0.940-6
0.3692	0.5	0.116-5	0.107-5	0.829-6	0.780-6
0.2692	0.4	0.941-6	0.850-6	0.667-6	0.615-6
0.1692	0.3	0.722-6	0.624-6	0.507-6	0.425-6

TABLE 4

SINGLE-PHOTON FREE-FREE CROSS SECTIONS

FOR ELECTRONS SCATTERED FROM THE GROUND

STATE OF ARGON

E_{phot} = 0.00882

E_{inc}	E_{fin}	Ar (exact)	Ar (soft)
0.99118	1.0	0.160+0	0.161+0
0.89118	0.9	0.142+0	0.143+0
0.79118	0.8	0.119+0	0.121+0
0.69118	0.7	0.960-1	0.970-1
0.59118	0.6	0.736-1	0.745-1
0.49118	0.5	0.534-1	0.544-1
0.39118	0.4	0.359-1	0.370-1
0.29118	0.3	0.213-1	0.224-1
0.19118	0.2	0.984-2	0.108-1
0.09118	0.1	0.239-2	0.305-2

Table 4. Single-Photon Free-Free Cross Sections for Electrons Scattered from the Ground State of Argon (Continued)

$E_{phot} = 0.086$

E_{inc}	E_{fin}	Ar (exact)	Ar (soft)
0.914	1.0	0.178-4	0.172-4
0.814	0.9	0.156-4	0.148-4
0.714	0.8	0.131-4	0.122-4
0.614	0.7	0.104-4	0.966-5
0.514	0.6	0.800-5	0.727-5
0.414	0.5	0.581-5	0.518-5
0.314	0.4	0.390-5	0.339-5
0.214	0.3	0.229-5	0.191-5
0.114	0.2	0.820-6	0.657-6

Table 4. Single-Photon Free-Free Cross Sections for Electrons Scattered from the Ground State of Argon (Continued)

$E_{phot} = 0.1308$

E_{inc}	E_{fin}	Ar (exact)	Ar (soft)
0.8692	1.0	0.334-5	0.335-5
0.7692	0.9	0.293-5	0.297-5
0.6692	0.8	0.245-5	0.251-5
0.5692	0.7	0.198-5	0.202-5
0.4692	0.6	0.152-5	0.155-5
0.3692	0.5	0.111-5	0.114-5
0.2692	0.4	0.753-6	0.783-6
0.1692	0.3	0.445-6	0.484-6

TABLE 5

DOUBLE-PHOTON FREE-FREE CROSS SECTIONS FOR ELECTRONS SCATTERED FROM THE METASTABLE STATES OF HELIUM

$E_{phot} = 0.00882$

E_{inc}	E_{fin}	^1S_o (exact)	^1S_o (soft)	$^3S_1$ (exact)	$^3S_1$ (soft)
0.98236	1.0	0.101-3	0.966-4	0.101-3	0.996-4
0.88236	0.9	0.941-4	0.909-4	0.947-4	0.935-4
0.78236	0.8	0.871-4	0.845-4	0.880-4	0.872-4
0.68236	0.7	0.796-4	0.777-4	0.809-4	0.802-4
0.58236	0.6	0.716-4	0.702-4	0.735-4	0.729-4
0.48236	0.5	0.631-4	0.621-4	0.656-4	0.652-4
0.38236	0.4	0.541-4	0.534-4	0.571-4	0.568-4
0.28236	0.3	0.444-4	0.441-4	0.478-4	0.476-4
0.18236	0.2	0.345-4	0.342-4	0.370-4	0.367-4
0.08236	0.1	0.230-4	0.226-4	0.206-4	0.203-4

Table 5. Double-Photon Free-Free Cross Sections for Electrons Scattered from the Metastable States of Helium (Continued)

$E_{phot} = 0.086$

E_{inc}	E_{fin}	^1S_o (exact)	^1S_o (soft)	^3S_o (exact)	$^3S_1$ (soft)
0.828	1.0	0.130-11	0.123-11	0.130-11	0.127-11
0.728	0.9	0.124-11	0.116-11	0.123-11	0.119-11
0.628	0.8	0.116-11	0.108-11	0.116-11	0.112-11
0.528	0.7	0.108-11	0.100-11	0.109-11	0.104-11
0.428	0.6	0.100-11	0.911-12	0.102-11	0.953-12
0.328	0.5	0.928-12	0.820-12	0.953-12	0.866-12
0.228	0.4	0.879-12	0.732-12	0.907-12	0.779-12
0.128	0.3	0.928-12	0.666-12	0.947-12	0.697-12
0.028	0.2	0.222-11	0.886-12	0.249-11	0.743-12

Table 5. Double-Photon Free-Free Cross Sections for Electrons Scattered from the Metastable States of Helium (Continued)

$E_{phot} = 0.1308$

E_{inc}	E_{fin}	^1S_o (exact)	^1S_o (soft)	$^3S_1$ (exact)	$^3S_1$ (soft)
0.7384	1.0	0.488-13	0.440-13	0.483-13	0.454-13
0.6384	0.9	0.465-13	0.416-13	0.464-13	0.429-13
0.5384	0.8	0.446-13	0.391-13	0.444-13	0.404-13
0.4384	0.7	0.426-13	0.364-13	0.426-13	0.378-13
0.3384	0.6	0.415-13	0.337-13	0.415-13	0.353-13
0.2384	0.5	0.420-13	0.315-13	0.422-13	0.329-13
0.1384	0.4	0.483-13	0.312-13	0.483-13	0.318-13
0.0384	0.3	0.108-12	0.484-13	0.119-12	0.407-13

TABLE 6

DOUBLE-PHOTON FREE-FREE CROSS SECTIONS

FOR ELECTRONS SCATTERED FROM THE GROUND

STATES OF HELIUM AND NEON

$E_{phot} = 0.00882$

E_{inc}	E_{fin}	He (exact)	He (soft)	Ne (exact)	Ne (soft)
0.98236	1.0	0.720-4	0.720-4	0.413-4	0.419-4
0.88236	0.9	0.608-4	0.607-4	0.325-4	0.329-4
0.78236	0.8	0.499-4	0.498-4	0.250-4	0.254-4
0.68236	0.7	0.395-4	0.395-4	0.187-4	0.190-4
0.58236	0.6	0.299-4	0.298-4	0.135-4	0.137-4
0.48236	0.5	0.211-4	0.211-4	0.930-5	0.943-5
0.38236	0.4	0.137-4	0.136-4	0.599-5	0.609-5
0.28236	0.3	0.761-5	0.759-5	0.345-5	0.351-5
0.18236	0.2	0.324-5	0.321-5	0.158-5	0.160-5
0.08236	0.1	0.697-6	0.692-6	0.372-6	0.381-6

Table 6. Double-Photon Free-Free Cross Sections for Electrons Scattered from the Ground States of Helium and Neon (Continued)

$E_{phot} = 0.086$

E_{inc}	E_{fin}	He (exact)	He (soft)	Ne (exact)	Ne (soft)
0.828	1.0	0.843-12	0.841-12	0.459-12	0.465-12
0.728	0.9	0.705-12	0.701-12	0.359-12	0.362-12
0.628	0.8	0.571-12	0.567-12	0.274-12	0.276-12
0.528	0.7	0.444-12	0.441-12	0.203-12	0.205-12
0.428	0.6	0.328-12	0.325-12	0.144-12	0.164-12
0.328	0.5	0.224-12	0.223-12	0.982-13	0.100-12
0.228	0.4	0.138-12	0.136-12	0.616-13	0.632-13
0.128	0.3	0.295-13	0.272-13	0.146-13	0.156-13

Table 6. Double-Photon Free-Free Cross Sections for Electrons Scattered from the Ground States of Helium and Neon (Continued)

$E_{phot} = 0.138$

E_{inc}	E_{fin}	He (exact)	He (soft)	Ne (exact)	Ne (soft)
0.7384	1.0	0.287-13	0.284-13	0.152-13	0.153-13
0.6384	0.9	0.238-13	0.235-13	0.118-13	0.119-13
0.5384	0.8	0.192-13	0.189-13	0.899-14	0.906-14
0.4384	0.7	0.148-13	0.145-13	0.663-14	0.671-14
0.3384	0.6	0.108-13	0.105-13	0.472-14	0.479-14
0.2384	0.5	0.728-14	0.705-14	0.319-14	0.327-14
0.1384	0.4	0.439-14	0.419-14	0.199-14	0.207-14
0.0384	0.3	0.255-14	0.226-14	0.118-14	0.129-14

TABLE 7

DOUBLE-PHOTON FREE-FREE CROSS SECTIONS

FOR ELECTRONS SCATTERED FROM THE GROUND

STATES OF CARBON AND NITROGEN

$E_{phot} = 0.00882$

E_{inc}	E_{fin}	C (exact)	C (soft)	N (exact)	N (soft)
0.98236	1.0	0.188-3	0.188-3	0.132-3	0.132-3
0.88236	0.9	0.153-3	0.153-3	0.106-3	0.106-3
0.78236	0.8	0.121-3	0.121-3	0.821-4	0.822-4
0.68236	0.7	0.905-4	0.907-4	0.610-4	0.612-4
0.58236	0.6	0.644-4	0.645-4	0.429-4	0.432-4
0.48236	0.5	0.424-4	0.424-4	0.280-4	0.282-4
0.38236	0.4	0.249-4	0.249-4	0.164-4	0.165-4
0.28236	0.3	0.122-4	0.122-4	0.804-5	0.817-5
0.18236	0.2	0.432-5	0.433-5	0.288-5	0.294-5
0.08236	0.1	0.726-6	0.729-6	0.428-6	0.511-6

Table 7. Double-Photon Free-Free Cross Sections for Electrons Scattered from the Ground States of Carbon and Nitrogen (Continued)

$E_{phot} = 0.086$

E_{inc}	E_{fin}	C (exact)	C (soft)	N (exact)	N (soft)
0.828	1.0	0.217-11	0.214-11	0.151-11	0.149-11
0.728	0.9	0.174-11	0.172-11	0.119-11	0.118-11
0.628	0.8	0.135-11	0.133-11	0.911-12	0.896-12
0.528	0.7	0.997-12	0.970-12	0.664-12	0.651-12
0.428	0.6	0.691-12	0.667-12	0.457-12	0.446-12
0.328	0.5	0.441-12	0.419-12	0.290-12	0.279-12
0.228	0.4	0.247-12	0.230-12	0.163-12	0.154-12
0.128	0.3	0.115-12	0.104-12	0.766-13	0.708-13
0.028	0.2	0.422-13	0.423-13	0.284-13	0.309-13

Table 7. Double-Photon Free-Free Cross Sections for Electrons Scattered from the Ground States of Carbon and Nitrogen (Continued)

$E_{phot} = 0.1308$

E_{inc}	E_{fin}	C (exact)	C (soft)	N (exact)	N (soft)
0.7384	1.0	0.741-13	0.714-13	0.511-13	0.493-13
0.6384	0.9	0.592-13	0.565-13	0.402-13	0.386-13
0.5384	0.8	0.456-13	0.431-13	0.306-13	0.291-13
0.4384	0.7	0.337-13	0.311-13	0.222-13	0.209-13
0.3384	0.6	0.234-13	0.211-13	0.153-13	0.141-13
0.2384	0.5	0.150-13	0.130-13	0.979-14	0.870-14
0.1384	0.4	0.887-14	0.708-14	0.578-14	0.486-14
0.0384	0.3	0.512-14	0.405-14	0.340-14	0.292-14

TABLE 8

DOUBLE-PHOTON FREE-FREE CROSS SECTIONS

FOR ELECTRONS SCATTERED FROM THE GROUND

STATE OF ARGON

$E_{phot} = 0.00882$

E_{inc}	E_{fin}	Ar (exact)	Ar (soft)
0.98236	1.0	0.333-3	0.333-3
0.88236	0.9	0.264-3	0.265-3
0.78236	0.8	0.192-3	0.192-3
0.68236	0.7	0.129-3	0.130-3
0.58236	0.6	0.806-4	0.811-4
0.48236	0.5	0.458-4	0.462-4
0.38236	0.4	0.228-4	0.232-4
0.28236	0.3	0.928-5	0.956-5
0.18236	0.2	0.263-5	0.248-5
0.08236	0.1	0.335-6	0.416-6

Table 8. Double-Photon Free-Free Cross Sections for Electrons Scattered from the Ground State of Argon (Continued)

$E_{phot} = 0.086$

E_{inc}	E_{fin}	Ar (exact)	Ar (soft)
0.828	1.0	0.371-11	0.372-11
0.728	0.9	0.281-11	0.279-11
0.628	0.8	0.196-11	0.194-11
0.528	0.7	0.128-11	0.126-11
0.428	0.6	0.772-12	0.750-12
0.328	0.5	0.418-12	0.405-12
0.228	0.4	0.193-12	0.188-12
0.128	0.3	0.687-13	0.703-13
0.028	0.2	0.159-13	0.216-13

Table 8. Double-Photon Free-Free Cross Sections for Electrons Scattered from the Ground State of Argon (Continued)

$E_{phot} = 0.1308$

E_{inc}	E_{fin}	Ar (exact)	Ar (soft)
0.7384	1.0	0.122-12	0.121-12
0.6384	0.9	0.905-13	0.881-13
0.5384	0.8	0.629-13	0.599-13
0.4384	0.7	0.406-13	0.379-13
0.3384	0.6	0.241-13	0.221-13
0.2384	0.5	0.128-13	0.116-13
0.1384	0.4	0.581-14	0.530-14
0.0384	0.3	0.213-14	0.237-14

SECTION IV

RESULTS AND CONCLUSIONS

It is convenient to examine our results from both qualitative and quantitative points of view. To address the first of these, we pose the question, "For radiative intensities up to 10^6 W-cm^{-2}, and frequencies at least as high as that of the CO_2 laser, what is the order of magnitude of the free-free cross section?" A rough answer can be had from the magnitude of the strength parameter that controls the relative rates of direct (no photons) and single quantum processes, namely $A_0^2/4c^2w^2$, where A_0 is the amplitude of the driving field's vector potential, c the speed of light, and w the optical angular frequency. At the CO_2 frequency and an intensity of 10^6 W-cm^{-2}, the indicated strength factor is 1.88×10^{-2}, and one anticipates that the radiative effect will represent a minor correction at this frequency. At the same intensity, the strength parameter has the values 2.08×10^{-7} and 3.9×10^{-8} at the wavelengths of the Nd+++ and ruby lasers, respectively, with the expectation of a negligible correction for these more energetic photons. These crude considerations were verified by detailed calculations performed with both realistic and unrealistic model potentials.

The calculations performed with the Kruger-Schulz close-coupling model supports our contention, even when Feshbach resonances are present and taken into account. Since this calculation has already been published (Ref. 9), we shall merely summarize our conclusions. The interested reader should refer to the paper for details, keeping in mind that the numerical values reported in Ref. 9 took the amplitude of the vector potential, A_0,

to be 1 atomic unit. To obtain single-photon cross sections at 10^6 W-cm^{-2}, the published cross sections should be multiplied by .0275. The analogous conversion factor for two-photon processes is $(.0275)^2 = 7.56 \times 10^{-4}$.

In general, non-resonant free-free cross sections for the CO_2 laser prove to be, in the Kruger-Schulz model, smaller than the corresponding radiationless cross sections by a factor of 100 or so, which is what one would expect on the crude basis discussed above. A similar ratio obtains for the relative magnitudes of non-radiative and radiative cross sections when there is a resonance. In that case, however, the non-radiative peak splits into two maxima when the radiation is on, occurring when either the initial or final electron energy is at the resonance. A splitting is evident in two-photon processes as well-this time there are three peaks, corresponding to a coincidence between the resonance and final, intermediate, and initial state electron energies. Of course, at the CO_2 wavelength, the two-photon transition rates are down by 10^{-2} from the single-photon rates, at our assumed intensity of 10^6 W-cm^{-2}.

That the resonance is split when the laser is on means that there will be energies for which the radiative process is resonant, while the direct is nonresonant, so that the free-free cross section could be larger than the (non-resonant) direct cross section at the same energy. This does not ordinarily mean, however, that in a plasma or other system with a broad energy distribution for the particles, that the photoabsorption process is competitive with direct excitation transfer. We shall discuss this point briefly.

In the plasma, if there is a resonance-enhanced cross section for a free-free process, there will be an enhanced, non-radiative process with

roughly 10^2 times the cross section, either at the same energy, or at an energy shifted by that of a photon. Evidently, if the electron energy distribution is flat, the radiative effect will be minor.

On the other hand, if the number density of electrons is a rapidly varying function of speed, one could envision a situation where there are many more electrons at a radiative resonance than at the corresponding non-radiative resonance, a feature that could compensate for the smaller cross section associated with the photoprocess. However, since the photon energy is about 0.1 eV, for this effect to be important, it would be necessary for the resonance to be near an excitation threshold at or near this energy. This condition does not seem to be satisfied for major laser-active atoms or molecules.

None of these questions arises at the higher frequencies where single quantum radiative cross sections are on the order of 10^{-7} of their non-radiative counterparts at intensities no larger than 10^6 W-cm^{-2}.

The order of magnitude of the radiative cross sections calculated with the realistic Robinson-Geltman potential is also small. Consequently, their actual numerical values are, in a sense, academic. We have decided to include them in this report, nevertheless, for several reasons. One might easily imagine going to higher intensities where free-free transitions might, in fact, be competitive with non-radiative processes. For these stronger fields, one might wish to have the actual numerical values, and, since they have been computed, it is reasonable to include them. At the CO_2 laser frequency, the radiative cross sections should be comparable to the direct at intensities of the order of 10^8 W-cm^{-2}, which represents only a relatively modest increase in power density over the

maximum assumed for the purposes of this report. Even the 10^{11}-10^{12} W-cm^{-2} required to make the photoabsorption rates at the ruby and Nd wavelengths comparable to direct transition rates is within the capabilities of those powerful solid-state lasers. Of course, at such intensity levels, other normally negligible effects will become important, as well as the free-free processes.

Secondly, the detailed calculations reveal general features of the laws governing the variation of free-free transition rates with relevant parameters, in particular the limits of validity of the soft-photon approximation. This is of particular value in view of the small number of experiments performed to date, and the difficulty of carrying these out. The exact numerical calculations serve as surrogates for experiments in testing approximations schemes.

We have calculated one- and two-photon free-free absorption cross sections at the frequencies of the CO_2, Nd+++, and ruby lasers, for targets consisting of the ground states of He, C, N, Ne, and Ar, and for the 1s2s metastable $^3S_1$ and $^1S_0$ states of He. Our results are exhibited in Tables 1 through 8, for electron energies in the range up to about 13 eV. In the Tables, the incident and final electron energies E_{inc}, E_{fin}, and E_{phot}, the photon energy, are in Rydberg units, and cross sections are expressed in a_0^2, where a_0 is the Bohr radius. Numerical values of cross sections are written in the form 0.xxx±n, where ±n is to be interpreted as a $10^{\pm n}$ multiplicative factor. Columns labeled "exact" and "soft" refer to exact numerical calculations in the model and the soft-photon approximation. The latter are evaluated using phase shifts determined numerically by solving the radial Schrodinger equation for the given target and electron energy.

All results represent total cross sections averaged over all orientations of the polarization, which is taken to be linear. No calculations for circularly polarized light are reported. Single photon cross sections are independent of the polarization state of the radiation, while model results indicate that the two-photon cross sections for circularly polarized light are very close to 2/3 of the linearly polarized cross sections over a wide range of conditions. (The ratio 2/3 holds exactly in the limit where the soft-photon approximation is valid.)

The realistic potential calculations are remarkably devoid of structure, but exhibit certain patterns. At the grossest level, we find that the extreme soft-photon approximation gives the correct order of magnitude for all the cross sections studied, but is quantitatively in error in some cases by as much as a factor of 3 or 4. We also find that the dependence of the free-free cross sections on electron energy differs according to whether the target is in the ground or metastable state. All of the cross sections for ground state targets increase with rising projectile energy in the range studied, varying by perhaps an order of magnitude in value. The behavior of the cross sections when the target is metastable helium is more varied. All of the single-photon cross sections decrease with increasing energy of the electrons, but, for fixed frequency, vary only by about a factor of two in the range investigated. The two-photon cross sections for the metastables conform to a different pattern. At the higher frequencies studied (the Nd+++ and ruby lasers), the cross sections initially diminish as the energy is increased, pass through a minimum, and then increase throughout the range. At the CO_2 laser frequency, the two-photon cross sections increase monotonically with electron energy throughout the Table.

The apparently anomalous behavior the metastable states exhibit is presumably not associated per se with the fact that they are excited, but rather with the large polarizabilities that they possess, and the concomitant presence of a bound s- and a bound or nearly bound p-state in the effective potential, both near zero energy. The ground states of the alkali atoms have similar properties, and we would expect these to more closely resemble the metastable levels of helium than the ground states studied.

That the two-photon cross section for the CO_2 wavelength and a metastable target increases with electron energy, while the other double-quantum cross sections pass through a minimum, can be understood qualitatively from the soft-photon approximation, although we recognize that this may be a poor method for getting quantitative results. In the soft-photon approximation, the differential cross section is proportional to the product of the corresponding radiationless cross section and D^{2n}, where D is the momentum transfer of the electron, and n the number of quanta absorbed or emitted. For the metastables, the radiationless cross section appears to decrease with projectile energy, a factor which dominates the dependence of the free-free cross section at low electron energies, except for the case of the two-photon problem at the CO_2 laser frequency, where the momentum transfer factor is particularly small for slow electrons.

The quality of agreement between the exact numerical cross sections and the results of the soft-photon approximation varies significantly from target to target. By far, the poorest agreement is obtained for the metastables. Among the ground state targets the soft-photon approximation

is least reliable for argon. As expected, the soft-photon results were closest to the exact calculations at the lowest frequency, that of the CO_2 laser.

That the soft-photon approximation was least reliable in the case of the metastables is understandable. The basic physical picture that describes the soft photon regime has the electron interacting with the radiation field for a long time, while the scattering occurs over a time scale that is short compared to an optical period. The shorter the scattering time, the better will be the soft photon approximation. In the case of the metastables, the scattering is dominated by the long range (r^{-4}) polarization potential, so that the collision time is relatively long. It is interesting to note that the two-photon cross sections for the metastables at 0.00882 Rydberg show much greater agreement between soft and exact results than do the single-photon cross sections. It is unclear why this is so, but we would speculate that it is associated with interference effects. We also note that the agreement between the soft and exact one-photon cross sections for the metastables improves as the electron energy decreases, which is opposite to what one would expect on the basis of the time-scale argument. This may be related to the observation of Spruch and co-workers (Ref. 13) that, for the radiationless scattering of a particle by a polarization potential, the first Born approximation becomes exact as the particle's energy is reduced to zero. We recall in this context the comment of Kruger and Schulz (Ref. 8), who point out that the soft-photon approximation is exact not only as the optical frequency goes to zero, but for all frequencies in the regime where the first Born approximation holds for the radiationless scattering.

As we have indicated, the poorest agreement for the ground state targets, between soft and exact cross sections, was obtained for argon. This may be related to the effective size of the atom, which is greatest for argon, which has an outermost 3p shell, while all the others have outermost 2p or 1s shells.

To summarize, we have performed calculations for free-free processes which indicate that, for laser intensities up to 10^6 W-cm^{-2}, radiatively assisted excitation mechanisms do not provide major corrections to their non-radiative counterparts. We have also compared the calculations performed with the soft-photon approximation with those performed by exact numerical methods, and find that the soft-photon results are most accurate for compact targets, and least accurate, in general, for highly polarizable atoms.

REFERENCES

(1) Gavrila, M. and van der Wiel, M. J.: "Free-Free Radiative Transitions of Electron-Atom Systems," Comments on Atomic and Molecular Physics 8, 1 (1978).

(2) Rosenberg, L.: "Theory of Electron-Atom Scattering in a Radiation Field," Advances in Atomic and Molecular Physics 18, 1 (1982).

(3) Mittleman, M. H.: "Resonant Potential Scattering in a Low-Frequency Laser Field," Phys. Rev. A 20, 1965 (1979).

(4) Weingartshofer, A., Holmes, J. K., Caudle, G., Clarke, E. M., and Kruger, H.: "Direct Observation of Multiphoton Processes in Laser-Induced Free-Free Transitions," Phys. Rev. Letters 39, 269, (1977).

(5) Langendam, P. J. K., Gavrila, M., Kaandorp, J. P. L., and van der Wiel, M. J.: "Resonant Free-Free Absorption by Electrons in the field of a Neon Atom," J. Phys. B 9 L453 (1976).

(6) Geltman, S.: "Free-Free Radiation in Electron-Neutral Atom Collisions," J. Quant, Spect. Rad. Transfer 13, 601 (1973).

(7) Robinson, E. J. and Geltman, S.: "Single and Double Quantum Photodetachment of Negative Ions", Phys. Rev. 153, 4 (1967).

8. Kruger, H. and Schulz, M.: "Laser-Induced Free-Free Electronic Transitions Near a Resonance," J. Phys. B 9, 1899 (1976).

(9) Shakeshaft, R. and Robinson, E. J.: "Free-Free Electron Scattering From a Model Atom: Comparison of One-Versus Two-Photon Absorption and Test of the Soft-Photon Approximation," Phys. Rev. A 25, 1977 (1982).

(10) Herman, F. and Skillman, S.: "Atomic Structure Calculations," Prentice-Hall, Englewood Cliffs, New Jersey, (1963).

(11) Mandl, A.: "Electron Photodetachment Cross Section of the Negative Ion of Fluorine," Phys. Rev. A 3, 251 (1971).

(12) Rothe, D.: "Radiative Capture of Electrons by Chlorine, Bromine, and Iodine Atoms," Phys. Rev. 177, 93 (1969).

(13) O'Malley, T. F., Spruch, L., and Rosenberg, L.: "Modification of Effective-Range Theory in the Presence of a Long-Range (r^{-4}) Potential," J. Math. Phys. 2, 491 (1961).

U.S.Government Printing Office: 1986 646-067/40760

END

FILMED

5-86

DTIC